Performance Evaluation of a DDST Based SIMO SC System with PAPR Reduction

Toni Levanen, Jukka Talvitie and Markku Renfors
Department of Communications Engineering
Tampere University of Technology
P.O.Box 553, FIN-33101, Finland
Email: toni.levanen@tut.fi

***Abstract*—In this paper we concentrate on the symbol level peak to average power ratio (PAPR) increase caused by a data dependent superimposed pilot sequence. Because we add the pilot sequence on top of the user data symbols, the dynamic range of the transmitted signal may increase significantly. We propose the usage of a simple limiter in the transmitter and a hard symbol estimate based iterative estimator for the receiver. We show by simulations that if we allow a modest increase in the symbol level PAPR, the spectral efficiency of the data dependent superimposed pilot based system is better than the traditional time domain multiplexed pilot based system in a block fading channel.**

***Keywords*: data dependent superimposed pilots; iterative receiver; peak to average power ratio; throughput comparison**

I. Introduction

Channel estimation and equalisation are crucial parts of modern receiver architectures. As we aim for higher and higher spectral efficiencies, the number of time instances allocated for training in the traditional time domain multiplexed (TDM) systems should be minimised. At the moment, the superimposed (SI) pilots [1] are seen as a potential solution. SI pilots are added directly on top of the user data, and thus all time instances contain user data. In other words, by using SI pilots we can improve the spectral efficiency by allowing the user information to occupy the whole spectral region designed for communications. The downside is that the user information interferes greatly with the pilot sequence and that the user data symbol power to interference power ratio is decreased.

To overcome this problem of self interference, in [2] a data dependent superimposed training (DDST) method was presented. The basic idea is very simple. Because the cyclic pilot sequence has its energy concentrated on certain frequency bins, we set the user data frequency response to zero on these frequency bins. This equals with removing the cyclic mean of the user data symbol sequence in the time domain. Therefore there is no interference from the user data to the pilot symbols. This can be seen as frequency domain multiplexed (FDM) pilot based training, but the difference to the basic setup is that the signal spectrum is not widened because of the used SI training symbols. Similar approach was studied in [3], where also the PAPR problem was discussed without any solutions to decrease the PAPR created by the SI pilots.

This work is supported by the Tampere Graduate School in Information Science and Engineering (TISE) and by the Finnish Foundation for Technology Promotion (TES).

The DDST training method is suitable especially for wide band single carrier (SC) systems. With multicarrier systems this would mean that we lose some subcarriers for pilot symbols. The problem with the DDST is the increased peak to average power ratio (PAPR), which violates one of the main benefits of using SC transmission. We address this problem by simply limiting the peak amplitudes at symbol level before transmission. Then, in the receiver side, we have a simple feedback based on hard symbol estimates, which we use to estimate the missing cyclic mean and the limited amplitudes.

We have extended the model provided in [2] to our SC model with filter bank (FB) based receiver structure, presented in [4]. The channel estimates are obtained in time domain after which the sub-channel wise equalisation (SCE) is performed in the frequency domain (for more details, see [4] and references there in). The FB based receiver structure is used because it provides close to ideal linear equaliser performance, has good spectral containment properties and is equally applicable also to SC-FDMA (DFT-S-OFDMA) as used in 3GPP-LTE uplink.

This paper is structured as follows. First we present the used system model. Next, in Section III we briefly describe the used ML-LMMSE channel estimation scheme for DDST. In Section IV the throughput performance comparison of DDST and TDM training based systems is provided. Finally, in Section V conclusions and future topics are provided.

Notation: Superscripts T and H denote the transpose and Hermitian transpose operators, $\otimes$ refers to the Kronecker product and $\circ$ defines a continuous time convolution. For complex numbers $|z|$ defines the absolute value of z and $\arg(\cdot)$ gives the argument of a complex number. For a complex vector $\mathbf{z}$, $|\mathbf{z}| = [|z_0|, \ldots, |z_{N-1}|]$ defines an element wise absolute value operation. The statistical expectation is denoted by $E[\cdot]$. The $(N \times N)$ identity matrix is denoted by $\mathbf{I}_N$ and the $(M \times M)$ matrix of all ones by $\mathbf{1}_M$. Occasionally, $\mathbf{1}_M$ can refer also to a column vector of ones with length M, but this is always clear from the context or mentioned in the text. Finally, $\text{diag}(\mathbf{a}) = \text{diag}(a_0, \ldots, a_{N-1})$ is an $(N \times N)$ diagonal matrix whose nth main diagonal value is a_n. Matrices are denoted by boldface uppercase letters and vectors by boldface lowercase letters.

II. SYSTEM MODEL

The system design originates from the uplink assumption. Thus, the complexity of the transmitting end is kept as small as possible and most of the complexity is positioned to the receiving end. The very simple block level design of the transmitter is given in Fig. 1. The transmitter contains bit source, channel encoder, interleaver (represented by π function), symbol mapper, pilot insertion, peak amplitude limiter and the transmitter pulse shape filter.

Let us assume that our symbol mapper produces a vector of data symbols $\mathbf{d}$ from some finite alphabet $\mathcal{A}^N$, where N is the frame (vector) length. We will use a pilot sequence, $\mathbf{p}$, which has length N_p. The pilot sequence is an optimal channel independent (OCI) sequence that was defined in [5]. In addition, we assume that our frame length is an integer multiple of N_p, given as $N = N_c N_p$, where N_c is the number of cyclic copies per frame. With the DDST, we first remove the cyclic mean of the data vector. As shown in [2], this can be represented as

$$\mathbf{z} = (\mathbf{I} - \mathbf{J}_{Tx})\mathbf{d}, \qquad (1)$$

where $\mathbf{J}_{Tx} = (1/N_c)\mathbf{1}_{N_c} \otimes I_{N_p}$. Now the data dependent pilot sequence is given as $\mathbf{p}_d = -\mathbf{J}_{Tx}\mathbf{d}$. The symbol sequence including user data symbols, data dependent pilot sequence and the cyclic pilot sequence is given as $\mathbf{s} = \mathbf{d} + \mathbf{p}_d + \mathbf{p}_c = \mathbf{z} + \mathbf{p}_c$, where the cyclic pilot sequence is defined as $\mathbf{p}_c = \mathbf{1}_{N_c} \otimes \mathbf{p}$ and $\mathbf{1}_{N_c}$ is a vector of ones. This sequence, $\mathbf{s}$, is then inserted to the peak amplitude limiter from which the limited signal $\breve{\mathbf{s}}$ is obtained. Finally, we normalise the signal to have unity power to obtain transmitted symbols $\tilde{\mathbf{s}}$. We define the power of the data sequence to be $\sigma_d^2 = 1 - \gamma$ and the power of the known pilot sequence to be $\sigma_{p_c}^2 = \gamma$, where γ is the power normalisation factor defining the allocated power for transmitted user data symbols and known pilot sequence.

The peak amplitude limiter takes as the maximum allowed amplitude value, a_{max}, the maximum amplitude value of the used constellation $\mathcal{A}$, defined as $\{a_{max} = \max(|(d)|), d \in \mathcal{A}, \sigma_d^2 = 1\}$. Note that here a_{max} is related to the maximum amplitude of a symbol constellation whose average power is normalised to unity. We chose this amplitude value to have similar peak powers as with time domain multiplexed (TDM) pilot based system. Now we can define the limited symbol sequence as

$$\breve{s}(k) = \begin{cases} s(k), \text{ if } |s(k)| \leq a_{max}, \\ a_{max} \cdot exp(j\arg(s(k))), \text{ if } |s(k)| > a_{max}. \end{cases} \qquad (2)$$

Now we have an amplitude limited symbol sequence whose PAPR is closer to the original value related to the data symbol sequence $\mathbf{d}$. The peak amplitudes are now limited to the original value, whereas the average power of the sequence is slightly decreased. In the simulations presented in Section IV, the energy per bit over one sided noise power spectral density, E_b/N_0, is defined for the normalised average power. In Table I the different average and peak powers with and without normalisation and the related PAPR are given for each constellation. Averaged powers σ_s^2 and $\sigma_{\breve{s}}^2$ are obtained by averaging over 1000 frames.

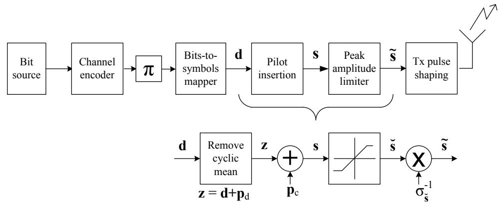

Fig. 1. Transmitter model.

TABLE I
SIMULATED POWER MEASURES FOR THE USED CONSTELLATIONS

	QPSK	16-QAM	64-QAM
σ_s^2	0.987	0.987	0.987
$\sigma_{\breve{s}}^2$	0.795	0.946	0.980
$max(\lvert s \rvert)^2$	2.419	3.405	3.760
$max(\lvert \breve{s} \rvert)^2$	1	1.8	2.33
$max(\lvert \tilde{s} \rvert)^2$	1.303	1.955	2.459
PAPR before limiter	2.451	3.464	3.805
PAPR after limiter	1.303	1.955	2.459
PAPR reduction (%)	46.8	43.6	35.4

By using a simple limiter in the transmitter we can remove most of the symbol level PAPR increase caused by cyclic mean removal and SI pilots. The QPSK modulation is the most sensitive to SI pilots because it originally has PAPR equal to one. Even after the limiter the symbol level PAPR is increased by 30.3%. 16-QAM and 64-QAM modulations are less sensitive and the remaining PAPR increase after the limiter is only 8.6% and 5.4%, respectively. Note that in this paper we have studied only the symbol level PAPR to provide some preliminary results on the limiter performance, and the true impact on the transmitted signal PAPR is left for future studies.

We define a vector $\mathbf{e}_{limiter} = \breve{\mathbf{s}} - \mathbf{s}$, which contains the information removed by the limiter from the sequence $\mathbf{s}$. In other words, it represents an additive error sequence generated by the limiter. In this paper we are not concerned with the estimation of the variance of this noise based on other system parameters, but this is an interesting problem for future studies. The error caused by the limiter is simply assumed to be zero mean complex Gaussian noise for complex constellations.

We assume a discontinuous block wise transmission where the channel is assumed to be time invariant during the transmission time of one block. The used channel model is ITU-R Vehicular A channel with about 2.5 μs delay spread and approximately 20 MHz bandwidth [6].

In Fig. 2 we have presented a block diagram of our multiantenna receiver. We assume perfect synchronization in frequency and time domain, ideal down conversion and 2 times oversampling of the received signal in Rx block. Based on these ideality assumptions, we can present the channel between transmitter and receiver as a 2 times oversampled discrete time equivalent channel as $h(k) = |h_{Tx}(t) \circ h_{channel}(t) \circ$

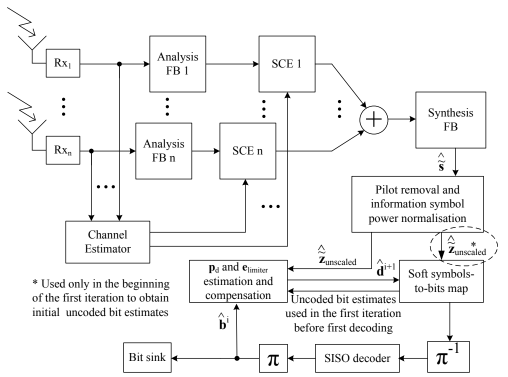

Fig. 2. Receiver model using multiantenna reception with maximum ratio combining and hard decision feedback loop for cyclic mean and limiter error estimation with DDST based channel estimation.

$h_{Rx}(t)|_{t=kT/2}$. The received symbol $y(k)$ can be given as

$$y(k) = \sum_{m=0}^{M-1} h(m)s(k-m) + w(k), \tag{3}$$

where M is the channel length in samples, k is the time index for 2 times oversampled symbol sequence and $s(k)$ is a transmitted symbol, which is zero if $k < 0$ or $k > 2N-1$. The noise term $w(k) = |h_{Rx}(t) \circ v(t)|_{t=kT/2}$, where $v(t)$ is complex additive white Gaussian noise (AWGN), is simply modelled as AWGN without considering the correlation caused by the 2 times oversampled receiver pulse shape filtering. Because of the oversampling, $s(k) = d(k) = p_c(k) = 0$ when k modulus 2 = 1. We will be more concentrated on the matrix notation of the signal model, which is given as

$$\mathbf{y} = \mathbf{H}\tilde{\mathbf{s}} + \mathbf{w} = \tilde{\mathbf{S}}\mathbf{h} + \mathbf{w}, \tag{4}$$

where the matrix $\tilde{\mathbf{S}} = \mathbf{D} + \mathbf{P}_d + \mathbf{P}_c + \mathbf{E}_{limiter}$ is built from the user data symbols, data dependent pilot sequence, known cyclic pilot sequence and the additive error generated by the limiter, respectively.

Because we assume a discontinuous block wise transmission, all matrices $\mathbf{D}, \mathbf{P}_d, \mathbf{P}_c$ and $\mathbf{E}_{limiter}$ have the form

$$\begin{bmatrix} x_0 & 0 & \cdots & 0 & 0 \\ x_1 & x_0 & \cdots & 0 & 0 \\ \vdots & \vdots & \ddots & \vdots & \vdots \\ x_{N_p-1} & x_{N_p-2} & \cdots & x_1 & x_0 \\ \vdots & \vdots & \ddots & \vdots & \vdots \\ x_{N-1} & x_{N-2} & \cdots & x_{N-N_p+1} & x_{N-N_p} \\ \vdots & \vdots & \ddots & \vdots & \vdots \\ 0 & 0 & \cdots & 0 & x_{N-1} \\ 0 & 0 & \cdots & 0 & 0 \end{bmatrix}, \tag{5}$$

including the zeros before and after the transmitted frame. Note that the matrices are now of dimension $(N + N_p \times N_p)$ and that we have assumed that $M = N_p$. This means that in the receiver we have to do the cyclic mean calculation over $N_c + 1$ copies. Thus, the cyclic mean of the received sequence is given as

$$\begin{aligned} \hat{\mathbf{m}}_y &= \mathbf{J}_{Rx}\mathbf{y} \\ &= (\mathbf{J}_{Rx}\mathbf{D} + \mathbf{J}_{Rx}\mathbf{P}_d + \mathbf{J}_{Rx}\mathbf{P}_c + \mathbf{J}_{Rx}\mathbf{E}_{limiter})\mathbf{h} + \mathbf{J}_{Rx}\mathbf{w} \\ &= \mathbf{P}\mathbf{h} + \hat{\mathbf{M}}_{e_{limiter}}\mathbf{h} + \hat{\mathbf{m}}_w, \end{aligned} \tag{6}$$

where $\mathbf{J}_{Rx} = (1/N_c)\mathbf{1}_{N_c \times N_c+1} \otimes I_{N_p}$ and $\hat{\mathbf{m}}_x$ defines the approximated cyclic mean vector of vector $\mathbf{x}$. Here $\hat{\mathbf{M}}_{e_{limiter}}$ is a matrix built from different cyclic shifts of $\hat{\mathbf{m}}_{e_{limiter}}$ and $\mathbf{P}$ is a cyclic matrix built from the OCI pilot sequence $\mathbf{p}$.

From the receiver frontend, the oversampled signal is provided for channel estimator and for analysis FB. The channel estimation algorithm to be defined in Section III is for one receiver branch and is simply repeated for each diversity branch. Here the channel equalisation of different branches can be done by either parallel or sequential processing. After obtaining channel estimate, SCE is performed in the frequency domain. It should be noted that the equalisation is now performed within mildly frequency selective subbands. More details on the equaliser structure can be found from [4] and references there in.

After SCE, different antenna branches are added together subsignal wise according to the maximum ratio combining principle. The composite subsignals are then recombined in the synthesis FB, which also efficiently realises the 2 times down conversion of the sampling rate. After the synthesis FB, the received sequence power is normalised to $1 + \sigma_w^2$, which corresponds to the total received power. We have assumed that we exactly know the noise variance in the receiver. After received power normalisation we remove the cyclic mean of the received sequence and normalise it based on the pilot power allocation. Thus, we obtain an estimate for the $\mathbf{z}$ with cyclic mean equal to zero and including the limiter error, given as

$$\hat{\tilde{\mathbf{z}}} = \sqrt{\frac{1}{1-\gamma}}(\mathbf{I} - \mathbf{J}_{\mathbf{Tx}})\sqrt{\frac{1+\sigma_w^2}{\sigma_{\hat{\tilde{s}}}^2}}\hat{\tilde{\mathbf{s}}}. \tag{7}$$

We have used the same notation for the vectors containing the same data but with different sampling rate. This is for the sake of clarity and should not cause any problems for the reader. The vectors before the analysis filter banks in Fig. 2 are related to 2 times oversampled sequences and the vectors after the synthesis filter bank are related to sequences sampled at the symbol frequency.

Next, we generate initial hard symbol estimates based on the *Soft symbols-to-bits* block output and use them for initial $\mathbf{p}_d$ and $\mathbf{e}_{limiter}$ estimation in the $\mathbf{p}_d$ *and* $\mathbf{e}_{limiter}$ *estimation and compensation* block. This block is presented in more detail in Fig. 3. This uncoded estimation of the cyclic mean and data dependent pilot signal is similar to one iteration of the hard, uncoded feedback algorithm proposed already in [2]. As a result, we have rough estimates of $\sigma_{\hat{\tilde{s}}}$, $\mathbf{p}_d$ and $\mathbf{e}_{limiter}$ available in the second soft symbols-to-bits mapping. Note that everything described above takes place before the first soft decoding process. This preprocessing phase causes

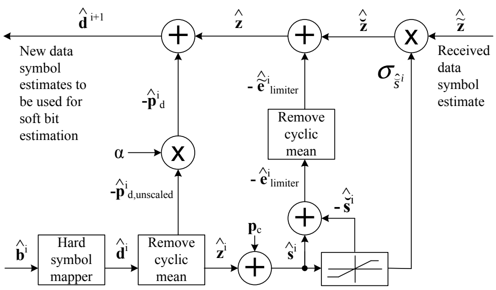

Fig. 3. A block diagram presenting the operations performed inside the $\mathbf{p}_d$ *and* $\mathbf{e}_{limiter}$ *estimation and compensation* block.

an insignificant increase in the receiver complexity, but does improve the quality of the first soft bit estimates provided for the soft decoder.

The soft bit estimates are then provided to the Turbo decoder (denoted as SISO decoder in Fig. 2). After the turbo decoding first bit estimates are provided for BER evaluation and this is considered to be the first iteration. The first iteration is not considered as a feedback iteration in our results.

In Fig. 3 subscript i refers to the iteration number and we have used notation $\hat{\hat{\mathbf{z}}}$ to represent our estimates of the data symbol sequence with cyclic mean set to zero and including the limiter error obtained from the *Pilot removal and information symbol power normalisation* block. First we generate hard symbol estimates based on the latest bit estimates $\hat{\mathbf{b}}^i$. Then we calculate the symbol wise cyclic mean and remove it from the symbol sequence. Next, we add the known pilot sequence on top of the symbol sequence $\hat{\mathbf{z}}^i$ and provide this sequence to the amplitude limiter. Then we calculate the limiter error estimate based on the input and the output of the limiter function.

Because we used power scaling in the transmitter, we approximate this normalisation factor in the receiver and use it to obtain normalised estimates $\hat{\hat{\mathbf{z}}} = \sigma_{\hat{\tilde{s}}^i}\hat{\hat{\mathbf{z}}}$. Next, we remove the latest limiter error estimates with cyclic mean removed to get $\hat{\mathbf{z}} = \hat{\hat{\mathbf{z}}} - \hat{\hat{\mathbf{e}}}^i_{limiter}$. We remove the cyclic mean from the limiter error estimates because it was also removed from our symbol estimates $\hat{\hat{\mathbf{z}}}$ in the *Pilot removal and information symbol power normalisation* block.

Next, we remove an normalised version of the latest data dependent pilot sequence $\hat{\mathbf{p}}^i_d = \alpha\hat{\mathbf{p}}^i_{d,unscaled}$ from $\hat{\mathbf{z}}$ to finally obtain our new unscaled data symbol estimates $\hat{\mathbf{d}}^{i+1}$. The power scaling factor for data dependent pilot sequence is given as

$$\alpha = \sqrt{\frac{E[|p_d|^2]}{\sigma^2_{\hat{p}^i_{d,unscaled}}}} = \sqrt{\frac{\sigma_d^2/N_c}{\sigma^2_{\hat{p}^i_{d,unscaled}}}}, \quad (8)$$

and it is used because typically during the first iterations the estimated cyclic mean has a too small variance. We know that the expected variance of the cyclic mean should be $E[|p_d|^2] = \sigma_d^2/N_c$, and therefore we use this normalisation factor to improve the performance.

III. ML-LMMSE Channel Estimation

When defining the LMMSE channel estimator, we want to minimise the expected value of the squared error, $E\{|\mathbf{h} - \hat{\mathbf{h}}|^2\}$. If we now make the assumptions that the noise and the total interference experienced by the pilot sequence is AWGN, channel taps are i.i.d. and have zero mean, i.e. $E\{\mathbf{h}\} = \mathbf{0}$, the LMMSE estimator can be simplified to [7]

$$\hat{\mathbf{h}} = (\sigma_w^2 \mathbf{C}^{-1}_{\hat{\mathbf{h}}_{apriori}} + \mathbf{P}_c^H\mathbf{P}_c)^{-1}\mathbf{P}_c^H\mathbf{y}, \quad (9)$$

where σ_w^2 is the AWGN channel noise. The channel covariance matrix $\mathbf{C}_{\mathbf{h}_{apriori}}$, contains the apriori information of the channel tap values. The apriori information of the channel taps are obtained through a ML channel estimator, defined as

$$\hat{\mathbf{h}}_{ML} = \frac{\mathbf{P}^H}{N_p\sigma_p^2}\hat{\mathbf{m}}_y. \quad (10)$$

By the assumption of independent tap coefficients, it becomes diagonal, i.e., $\mathbf{C}_{\hat{\mathbf{h}}_{ML}} = diag\{|\hat{h}(0)|^2, |\hat{h}(1)|^2, \cdots, |\hat{h}(N_p - 1)|^2\}$. By assuming the cyclic OCI training sequence, the LMMSE estimator can be reduced to

$$\hat{\mathbf{h}}_{ML-LMMSE} = \left(\frac{\sigma_w^2}{N_c}\mathrm{diag}(|\hat{\mathbf{h}}_{ML}|^{-2}) + N_p\sigma_p^2 I_{N_p}\right)^{-1}\mathbf{P}^H\hat{\mathbf{m}}_y. \quad (11)$$

With DDST, the ML channel estimate is quite good, but we can further improve it by using the LMMSE channel estimator following the ML channel estimator. For this reason, the channel estimator is named as ML-LMMSE. Another reason to use ML-LMMSE structure is to compensate for the additional error caused by the limiter error present in the signal. It would probably improve the estimation performance if we could provide an limiter error variance estimate for the channel estimator, but this is left for future studies. This kind of channel estimator structure with traditional SI pilots and iterative interference cancelling feedback was studied in [8].

IV. Simulated Throughput Performance Comparison Between DDST and TDM Based Training

The used channel model is ITU-R Vehicular A channel with about 2.5 μs delay spread and approximately 20 MHz bandwidth [6]. The delay spread is 78 samples in the receiver, where 2 times oversampling is used in the analysis filter bank. The oversampling allows us to efficiently realise the RRC filtering in frequency domain combined in the channel equalisation process. More details can be found, e.g., [4] and references there in.

The channel codec is a turbo codec with generator matrix $G = \left[1\ \frac{1\,5}{1\,3}\right]$. The used interleavers are bitwise S-interleavers, where the distance parameter is defined as $S = \sqrt{L/2}$, where L is the length of the unit which is interleaved. In channel interleaving the unit is the whole transmitted frame and inside a turbo encoder/decoder the interleaving unit one code block. Each transmitted frame is divided into Q coded blocks, where 2^Q defines the used constellation size.

TABLE II
SIMULATION PARAMETERS

Symbol rate	15.36 MHz
Signal bandwidth	18.74 MHz
Frame duration	250 μs
Order of the RRC filter	32
RRC roll-off	0.22
Symbols per frame	3840
TDM pilot symbols per frame	384
γ with 4-QAM	0.1
γ with 16-QAM	0.05
γ with 64-QAM	0.02
No. of subbands in the analysis FB	256
No. of subbands in the synthesis FB	128
Overlapping factor	5
FB roll-off	1

We have run the simulations for QPSK, 16-QAM and 64-QAM constellations with code rates $R = 0.5$, $R = 0.67$ and $R = 0.75$. Puncturing is performed over parity bits. Some additional simulation parameters related to the simulation model are given in Table II. For DDST, the SI pilot powers were defined for each constellation by choosing the pilot power leading to the smallest average BER with three feedback iterations (in total four iterations). The averaging was done over all code rates and with 2 and 4 receiving antennas. These results could have been further optimized by defining different pilot powers for each coding and receiving antenna number pair, but this is out of the scope of this paper.

In the Fig. 4 we have presented results for DDST with combined ML-LMMSE after three feedback iterations with increased symbol level PAPR and for TDM using also ML-LMMSE type equaliser. Furthermore, in the presented spectral efficiency figures, we have presented the spectral efficiency with our system if the channel response is known in the receiver and no pilots are transmitted. This represents an upper bound of the spectral efficiency for the given system. The provided results assume that the receiver knows exactly the noise variance and are derived by choosing the highest achievable rate among all code-constellation pairs for each E_b/N_0 point.

From Fig. 4 we can clearly see how the DDST based system improves the spectral efficiency if we allow increased symbol level PAPR. It should be noted, that the symbol level PAPR does not directly map to PAPR after the pulse shape filtering and this topic requires additional studies. The maximum spectral efficiency difference for each constellation is equal to 10%, which corresponds to the number of pilot symbols allocated for TDM. We could have used less TDM pilots with 4 receiving antennas, but we thought that this would not correspond to a real life scenario, where the transmitted frame structure is fixed regardless of the number of receiving or transmitting antennas.

V. CONCLUSION

In this paper we have presented a simple limiter approach to decrease the severe PAPR problem related to DDST in the transmitter. For the reception, a simple algorithm to estimate

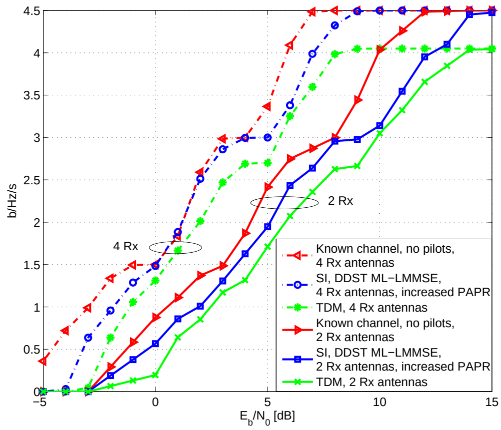

Fig. 4. Throughput performance comparison for DDST and TDM training based systems. In addition, performance without any pilots and known channel response is shown.

the additional error term caused by the limiter was presented. With the given system, spectral efficiency improvements can be achieved if we allow increased symbol level PAPR in the transmitter and increased reception complexity in the receiver. These results are preliminary, but they provide insight to the possibilities of DDST training in wireless communications.

In a coming article, the MSE performance bounds of the ML-LMMSE estimator with DDST will be presented. Further more, additional details on the the true transmitted signal PAPR, limiter error structure and their effects on the system performance will be provided.

REFERENCES

[1] P. Hoeher and F. Tufvesson, "Channel Estimation with Superimposed Pilot Sequence," in *Global Telecommunications Conference 1999, GLOBECOM '99*, vol. 4, 1999, pp. 2162–2166.

[2] M. Ghogho et al., "Channel Estimation and Symbol Detection for Block Transmission Using Data-Dependent Superimposed Training," *IEEE Signal Process. Lett.*, vol. 12, no. 3, pp. 226–229, 2005.

[3] C. Lam et al., "Channel Estimation for SC-FDE Systems Using Frequency Domain Multiplexed Pilots," in *IEEE 64th Vehicular Technology Conf., 2006, VTC-2006 Fall*, Montral, Canada, 25-28 Sept., pp. 1–5.

[4] Y. Yang, T. Ihalainen, M. Rinne and M. Renfors, "Frequency-domain Equalization in Single-carrier Transmission: Filter Bank Approach," *EURASIP Journal on Advances in Signal Processing*, vol. 2007, Article ID 10438, 16 pages, 2007.

[5] A. G. Orozco-Lugo, M. M. Lara, and D. C. McLernon, "Channel Estimation Using Implicit Training," *IEEE Trans. Signal Process.*, vol. 52, no. 1, pp. 240–254, 2004.

[6] T. B. Sorensen, P. E. Mogensen, and F. Frederiksen, "Extension of the ITU Channel Models for Wideband (OFDM) Systems," in *IEEE 62nd Vehicular Technology Conference 2005, VTC-2005-Fall*, Dallas, Texas USA, 25-28 Sept. 2005, pp. 392–396.

[7] M. Pukkila, "Iterative Receivers and Multichannel Equalisation for Time Division Multiple Access Systems," Ph.D. dissertation, Helsinki University of Technology, Espoo, Finland, 10 Oct. 2003, ISBN 951-22-6717-9.

[8] T. Levanen and M. Renfors, "Improved Performance Bounds for Iterative IC LMMSE Channel Estimator with SI Pilots," in *21st Annual IEEE International Symposium on Personal, Indoor and Mobile Radio Communications*, Istanbul, Turkey, 26-30 Sept. 2010.